MIXED CONVECTIVE RADIATIVE FLOW OF VISCOELASTIC LIQUID SUBJECT TO SPACE DEPENDENT INTERNAL HEAT SOURCE AND CHEMICAL REACTION

by

Tasawar HAYAT[a,b], Ikram ULLAH[a*], Ahmed Al-SAEDI[b], and Bashir AHMAD[b]

[a] Department of Mathematics, Quaid-I-Azam University, Islamabad, Pakistan
[b] Nonlinear Analysis and Applied Mathematics (NAAM) Research Group, Department of Mathematics, Faculty of Science, King Abdulaziz University, Jeddah, Saudi Arabia

Original scientific paper
https://doi.org/10.2298/TSCI171229287H

Present study addresses Soret and Dufour effects in mixed convection MHD flow of viscoelastic liquid with chemical reaction. Flow induced by an exponential stretching sheet is addressed in the presence of magnetic field. Energy expression is modelled by exponential space dependent internal heat source, thermal radiation, and convective condition. Relevant problems are modelled by employing boundary-layer concept. The partial differential systems are reduced to ordinary differential systems, and problem is solved by homotopic technique. Physical insight of results is arranged by graphs and tables.

Key words: *viscoelastic liquid, exponential based heat source, mixed convection, chemical reaction*

Introduction

Liquid flow over a stretched surface has been attracted by the engineers, and scientists devoted to numerical simulations and modeling. It is due to its vast applications in the manufacturing process and polymer industry comprising spinning of filaments, wire drawing, hot rolling, production of crystal growing fibers, processing of food stuffs, paper production, rapid spray cooling, continues casting, cooling of microelectronics and glass blowing. Crane [1] inspected the boundary-layer flow of an incompressible viscous fluid over a linear stretching sheet. He obtained similarity solution in closed form. Since then, many researchers [2-8] provided their research contributions via various concept of stretching surfaces. However, in fact the stretching of a plastic sheet may not essentially be linear. The characteristics of flow and heat transfer by an exponentially stretched surface is important for thinning and annealing of copper wires, food, paper and plastic processes. The final product depends critically on rate of heat transfer and stretching. Both kinematics of cooling or simultaneous heating and stretching have a crucial effect on the nature of final product [9]. Magyari and Keller [10] examined the flow due to an exponentially stretching sheet. They studied the heat transfer aspects in the case where the wall temperature varies exponentially from the leading edge. Viscous dissipation in mixed convective flow by an exponentially stretching surface is studied by Partha *et al.* [11]. It is found that velocity enhances for both mixed convection and viscous dissipation. Sajid and Hayat [12] explored

* Corresponding author, e-mail: ikram020@yahoo.com

radiation in flow by an exponentially stretching surface. Flow of magneto second grade nanoliquid persuaded by an exponentially stretching sheet discussed by Hayat *et al.* [13].

The respective mass/energy fluxes can be achieved by taking gradients of temperature/concentration. Thermal-diffusion (Soret effect) is generated because of temperature gradient while diffusion-thermo (Dufour effect) occurred due to concentration gradient. Such aspects have great implementation in area of chemical engineering and geosciences. Soret effect can be seen in solar ponds, micro-structure, and the biological systems of the world oceans. Thermal-diffusion is also utilized in process of isotope separation and in mixture between gases with small molecular weight (He, H_2) and of medium molecular weight (air, N_2). Related analysis in this direction have been mentioned by the studies [14-18].

Excessive heat generation is a serious issue in engineering applications like nuclear power plants, concrete industry, computer processors and inside of earth. Effective heat transfer can drastically improve the effectiveness in such cases. There is most likely that heat transfer is very valuable in dilution technique, dialysis, oxygenation, and hyperthermia. Tissue engineering uses thermal excursion to selectively destroy tissues and cells. All these applications require heat transfer in the most proficient way by utilizing both free and forced convection which frequently supports mass transfer too. Heat and mass transfer through mixed convection is noticeable in processes like food solidification, diffusion of nutrients, reverse osmosis, cooling of nuclear reactors, float glass production cell separation, chemical waste management, cooling of combustion chamber wall in a gas defroster and turbine system. Many researchers admits the importance of involvement of mixed convection. Mixed convection in MHD viscoelastic fluid flow over a porous stretching sheet is analytically elaborated by Turkyilmazoglu [19]. Mixed convective boundary-layer flow over a convectively heated sheet is addressed by Grosan *et al.* [20]. The MHD mixed convective flow by an inclined porous plate with slip effect is discussed by Das *et al.* [21]. Imtiaz *et al.* [22] studied mixed convective nanofluid flow with Newtonian heating. Hayat *et al.* [23] studied mixed convection in 3-D flow of Sisko nanoliquid. Further importance of thermal radiation is prevalent in the industrial and space technology process at very high temperature. Furnace design, plasma physics, space craft re-entry and propulsion system, satellites, nuclear plants, *etc.* are examples of such processes. In general radiation along with the free and forced convective flows is of crucial importance in space technology and high temperature processes. Human body sustains suitable temperature by considering these two procedures. Few studies for thermal radiation in the presence of mixed convection are given through refs. [24-28].

Here our motivation is to assess the outcome of exponential heat source in flow of viscoelastic liquid by an exponentially moving surface. Few investigators in the past only utilized exponential heat source [29-31]. There is no analysis available yet that looks flow of viscoelastic liquid with such aspect. Additionally, we accounted radiation, thermal diffusion and diffusion thermo (cross-diffusion) and chemical reaction. The governing problems are achieved via boundary-layer assumptions. Homotopic approach [32-43] is employed for the solutions of non-dimensional governing problems. Physics of sundry variables are studied graphically and for tabulated values.

Problems development

Consider 3-D mixed convection flow of an incompressible viscoelastic liquid. Exponentially stretching sheet induces the flow. Applied magnetic field is imposed along z-axis. Small magnetic Reynolds number is accounted. The laminar flow is restricted in the domain $z > 0$. Heat and mass transfer characteristics have been adopted when both Soret and Dufour

effects are present. Additionally, exponentially heat source and chemical reaction are addressed. Radiation is entertained in the energy expression. Moreover the respective sheet and ambient liquid temperatures and concentrations are designated through (T_f and T_∞), and (C_w and C_∞). Keeping the aforesaid assumptions in mind, the governing problems are:

$$\frac{\partial u}{\partial x}+\frac{\partial v}{\partial y}+\frac{\partial w}{\partial z}=0 \tag{1}$$

$$u\frac{\partial u}{\partial x}+v\frac{\partial u}{\partial y}+w\frac{\partial u}{\partial z}=\nu\frac{\partial^2 u}{\partial z^2}-k_0\left(\begin{array}{c}u\dfrac{\partial^3 u}{\partial x\partial z^2}+w\dfrac{\partial^3 u}{\partial z^3}-\dfrac{\partial u}{\partial x}\dfrac{\partial^2 u}{\partial z^2}-\\ -\dfrac{\partial u}{\partial z}\dfrac{\partial^2 w}{\partial z^2}-2\dfrac{\partial u}{\partial z}\dfrac{\partial^2 u}{\partial x\partial z}-2\dfrac{\partial w}{\partial z}\dfrac{\partial^2 u}{\partial z^2}\end{array}\right)-$$

$$-\frac{\sigma B_0^2}{\rho}u+\mathrm{g}\left[\beta_T(T-T_\infty)+\beta_C(C-C_\infty)\right] \tag{2}$$

$$u\frac{\partial v}{\partial x}+v\frac{\partial v}{\partial y}+w\frac{\partial v}{\partial z}=\nu\frac{\partial^2 v}{\partial z^2}-k_0\left(\begin{array}{c}v\dfrac{\partial^3 v}{\partial x\partial z^2}+w\dfrac{\partial^3 v}{\partial z^3}-\dfrac{\partial v}{\partial y}\dfrac{\partial^2 v}{\partial z^2}-\\ -\dfrac{\partial v}{\partial z}\dfrac{\partial^2 w}{\partial z^2}-2\dfrac{\partial v}{\partial z}\dfrac{\partial^2 v}{\partial x\partial z}-2\dfrac{\partial w}{\partial z}\dfrac{\partial^2 v}{\partial z^2}\end{array}\right)-\frac{\sigma B_0^2}{\rho}v \tag{3}$$

$$u\frac{\partial T}{\partial x}+v\frac{\partial T}{\partial y}+w\frac{\partial T}{\partial z}=\alpha_m\frac{\partial^2 T}{\partial z^2}+\frac{Dk_T}{c_s c_p}\frac{\partial^2 C}{\partial z^2}-\frac{1}{\rho c_p}\frac{\partial q_r}{\partial z}+$$

$$+Q_0\frac{(T_w-T_\infty)}{\rho c_p}\exp\left[-\left(\frac{U_0}{2\nu L}\right)^{1/2}\mathrm{e}^{\frac{x+y}{2L}}z\right] \tag{4}$$

$$u\frac{\partial C}{\partial x}+v\frac{\partial C}{\partial y}+w\frac{\partial C}{\partial z}=D\frac{\partial^2 C}{\partial z^2}+\frac{Dk_T}{T_m}\frac{\partial^2 T}{\partial z^2}-K_m(C-C_\infty) \tag{5}$$

$$u=U_w,\quad v=V_w,\quad w=0,\quad k\frac{\partial T}{\partial z}=h_f(T_f-T),\quad C=C_w\quad\text{at}\quad z=0 \tag{6}$$

$$u\to 0,\quad v\to 0,\quad T\to T_\infty,\quad C\to C_\infty\quad\text{as}\quad z\to\infty \tag{7}$$

where (u, v, w) denote the respective velocity components parallel to (x, y, z), $k_0=-\alpha_1/\rho$ – the elastic parameter with $k_0>0$ represents elastico-visous liquid, $k_0<0$ for second grade fluid and $k_0=0$ for viscous liquid, α_1 – the normal stress moduli, Q_0 – the heat generation/absorption variable, $\nu=\mu/\rho$ – the kinematic viscosity, ρ – the density, g – the acceleration due to gravity, μ – the dynamic viscosity, β_C – the coefficient of solutal expansion, T – the temperature, β_T – the coefficient of thermal expansion, α_m – the thermal diffusivity, k_T – the thermal-diffusion, D – the diffusion coefficient, c_p – the specific heat, T_m – the fluid mean temperature, q_r – the radiative heat flux, C – the concentration, c_s – the concentration susceptibility, K_m – the chemical reaction rate, and h_f – the convective heat transfer coefficient. This analysis presumes that surface stretching velocities, wall temperature and concentration are:

$$U_w=U_0\mathrm{e}^{\frac{x+y}{L}},\quad V_w=V_0\mathrm{e}^{\frac{x+y}{L}},\quad T_w=T_f=T_\infty+T_0\mathrm{e}^{\frac{A(x+y)}{2L}},\quad C_w=C=C_\infty+C_0\mathrm{e}^{\frac{B(x+y)}{2L}} \tag{8}$$

where U_0, V_0, T_0, and C_0 are the constants, A is the temperature exponent, B is the concentration exponent, and L is the reference length. Through Rosseland's approximation the expression for radiative heat flux q_r is:

$$q_r = -\frac{4\sigma_1}{3m^{**}}\frac{\partial(T^4)}{\partial y} = -\frac{16\sigma^{**}T_\infty^3}{3m^{**}}\frac{\partial^2 T}{\partial z^2} \tag{9}$$

in which σ^{**} shows the Stefan-Boltzman and m^{**} designates the coefficient of mean absorption. Invoking eq. (9) the energy equation can be converted to the form:

$$u\frac{\partial T}{\partial x} + v\frac{\partial T}{\partial y} + w\frac{\partial T}{\partial z} = \alpha_m\frac{\partial^2 T}{\partial z^2} + \frac{Dk_T}{c_s c_p}\frac{\partial^2 C}{\partial z^2} + \frac{16\sigma_1 T_\infty^3}{3m\rho c_p}\frac{\partial^2 T}{\partial z^2} + \\ + Q_0\frac{(T_w - T_\infty)}{\rho c_p}\exp\left[-\left(\frac{U_0}{2\nu L}\right)^{1/2} \mathrm{e}^{\frac{x+y}{2L}} z\right] \tag{10}$$

The dimensionless variables are taken in the forms:

$$u = U_0\mathrm{e}^{\frac{x+y}{L}} f'(\eta),\ \ v = U_0\mathrm{e}^{\frac{x+y}{L}} g'(\eta),\ \ w = -\left(\frac{\nu U_0}{2L}\right)^{1/2} \mathrm{e}^{\frac{x+y}{2L}}\left(f + \eta f' + g + \eta g'\right) \\ T = T_\infty + T_0\mathrm{e}^{\frac{A(x+y)}{2L}}\theta(\eta),\ \ C = C_\infty + C_0\mathrm{e}^{\frac{B(x+y)}{2L}}\phi(\eta),\ \ \eta = \left(\frac{U_0}{2\nu L}\right)^{1/2} \mathrm{e}^{\frac{x+y}{2L}} z \tag{11}$$

Equation (1) is identically satisfied while the eqs. (2)-(8) and eq. (10) give:

$$f''' + (f+g)f'' - 2(f'+g')f' + K\begin{bmatrix} 6f'''f' + (3g'' - 3f'' + \eta g''')f'' + \\ +(4g' + 2\eta g'')f''' - (f + g + \eta g')f'''' \end{bmatrix} - \\ -M^2 f' + 2\lambda(\theta + N\phi) = 0 \tag{12}$$

$$g''' + (f+g)g'' - 2(f'+g')g' + K\begin{bmatrix} 6g'''g' + (3f'' - 3g'' + \eta f''')g'' + \\ +(4f' + 2\eta f'')g''' - (f + g + \eta f')g'''' \end{bmatrix} - M^2 g' = 0 \tag{13}$$

$$(1 + Rd)\theta'' + \mathrm{Pr}[(f+g)\theta' - A(f'+g')\theta + D_f\phi'' + \delta\exp(-\eta)] = 0 \tag{14}$$

$$\phi'' + \mathrm{Sc}[(f+g)\phi' - B(f'+g')\phi + \mathrm{Sr}\,\theta'' - \gamma_1\phi] = 0 \tag{15}$$

$$f = 0,\ \ g = 0,\ \ f' = 1,\ \ g' = \alpha,\ \ \theta' = -\gamma[1 - \theta(0)],\ \ \phi' = 1 \ \text{ at } \ \eta = 0 \tag{16}$$

$$f' \to 0,\ \ g' \to 0,\ \ \theta \to 0,\ \ \phi \to 0 \ \text{ as } \ \eta \to \infty \tag{17}$$

where λ shows mixed convection variable, K – the dimensionless viscoelastic parameter, M – the magnetic parameter, δ – the heat source parameter, N – the buoyancy ratio, Gr – the Grashof number, Re – the Reynold number, α – the ratio parameter, Rd – the radiation parameter, D_f – the Dufour number, Pr – the Prandtl number, Sr – the Soret number, Sc – the Schmidt number, γ – the Biot number due to temperature, and γ_1 – the chemical reaction parameter. These quantities have values:

$$\lambda=\frac{\mathrm{Gr}}{\mathrm{Re}^2},\ N=\frac{\beta_C\left(C_w-C_\infty\right)}{\beta_T\left(T_w-T_\infty\right)},\ \mathrm{Gr}=\frac{\mathrm{g}\beta_T(T_w-T_\infty)}{\nu^2},\ \mathrm{Re}=\frac{U_wL}{\nu},\ \alpha=\frac{V_0}{U_0},\ K=\frac{k_0U_w}{2\nu L}$$
$$\mathrm{Pr}=\frac{\nu}{\alpha_m},\ Rd=\frac{16\sigma_1T_\infty^3}{3km},\ D_f=\frac{Dk_T}{c_sc_p\nu}\frac{(C_w-C_\infty)}{(T_w-T_\infty)},\ \mathrm{Sc}=\frac{\nu}{D},\ \mathrm{Sr}=\frac{Dk_T}{T_m\nu}\frac{(T_w-T_\infty)}{(C_w-C_\infty)} \tag{18}$$
$$\gamma=\frac{h}{k}\sqrt{\frac{2\nu L}{U_w}},\ \gamma_1=\frac{K_mL}{U_0},\ \delta=\frac{Q_0L}{U_0\rho c_p},\ M^2=\frac{2\sigma B_0^2L}{\rho U_w}$$

Expressions for local Nusselt number, Nu_x, and Sherwood, Sh_x, numbers are stated as:

$$\mathrm{Nu}_x=\frac{xq_w}{k(T_w-T_\infty)}+(q_r)_w,\ \mathrm{Sh}_x=\frac{xj_w}{D(C_w-C_\infty)} \tag{19}$$

where

$$q_w=-k\left(\frac{\partial T}{\partial z}\right)_{z=0},\quad j_w=-D\left(\frac{\partial C}{\partial z}\right)_{z=0} \tag{20}$$

Equations (19)-(20) in non-dimensional form gives:

$$\left(\frac{\mathrm{Re}_x}{2}\right)^{-1/2}\mathrm{Nu}_x=-\frac{x}{L}\left(1+Rd\right)\theta'(0) \tag{21}$$

$$\left(\frac{\mathrm{Re}_x}{2}\right)^{-1/2}\mathrm{Sh}_x=-\frac{x}{L}\phi'(0) \tag{22}$$

where $\mathrm{Re}=U_wL/\nu$ defines the Reynolds number.

Analysis of series solutions

The initial approximations ($f_0,\ g_0,\ \theta_0,\ \phi_0$) and operators ($\overline{\mathbf{L}}_f,\ \overline{\mathbf{L}}_g,\ \overline{\mathbf{L}}_\theta,\ \overline{\mathbf{L}}_\phi$) are:

$$f_0(\eta)=1-\mathrm{e}^{-\eta},\quad g_0(\eta)=\alpha(1-\mathrm{e}^{-\eta})$$
$$\theta_0(\eta)=\frac{\gamma}{1+\gamma}\mathrm{e}^{-\eta},\quad \phi_0(\eta)=\frac{\gamma_1}{1+\gamma_1}\mathrm{e}^{-\eta} \tag{23}$$
$$\overline{\mathbf{L}}_f=f'''-f',\quad \overline{\mathbf{L}}_g=g'''-g'$$
$$\overline{\mathbf{L}}_\theta=\theta''-\theta,\quad \overline{\mathbf{L}}_\varphi=\phi''-\phi \tag{24}$$

with

$$\overline{\mathbf{L}}_f\left[\beta_1^{**}+\beta_2^{**}\mathrm{e}^{\eta}+\beta_3^{**}\mathrm{e}^{-\eta}\right]=0,\quad \overline{\mathbf{L}}_g\left[\beta_4^{**}+\beta_5^{**}\mathrm{e}^{\eta}+\beta_6^{**}\mathrm{e}^{-\eta}\right]=0$$
$$\overline{\mathbf{L}}_\theta\left[\beta_7^{**}\mathrm{e}^{\eta}+\beta_8^{**}\mathrm{e}^{-\eta}\right]=0,\quad \overline{\mathbf{L}}_\phi\left[\beta_9^{**}\mathrm{e}^{\eta}+\beta_{10}^{**}\mathrm{e}^{-\eta}\right]=0 \tag{25}$$

in which β_i^{**} (i = 1-10) depict the constants.

Here it is desired to achieve the admissible ranges of embedding variables for convergence of series solutions. For such intention, we have sketched the $\hbar$ curves, fig. 1. Clearly these figures depict that acceptable values of these embedding variables are $-0.65\le\hbar_f\le-0.09$, $-0.64\le\hbar_g\le-0.01$, $-1.03\le\hbar_\theta\le0.1$, and $-0.98\le\hbar_\phi\le0.1$.

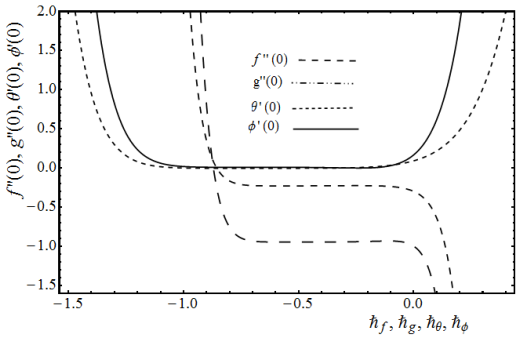

Figure 1. The $\hbar$ -curves for $f(\eta)$, $g(\eta)$, $\theta(\eta)$, and $\phi(\eta)$

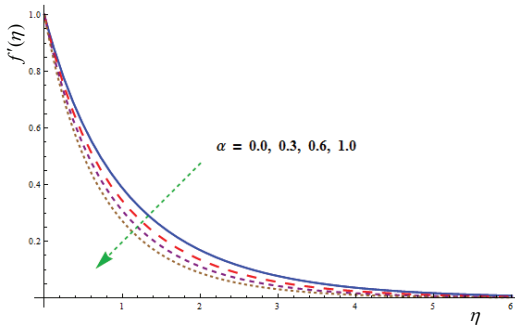

Figure 2. Impact of $f'(\eta)$ via α

Discussion

Main emphasis here is given to address the salient feature of influential parameters on velocities, temperature and concentration. The responses of Nusselt and Sherwood numbers for distinct values of interesting variables are examined, see tab. 1. Aspects of α on $f'(\eta)$ and $g'(\eta)$ are portrayed in figs. 2 and 3. Here velocity components $f'(\eta)$ and $g'(\eta)$ show reverse trend when α is enhanced. Physically when α increases from zero then lateral surface begins to expand in the *y*-direction and it shrink in *x*-direction. Thus $g'(\eta)$ increases while the velocity components $f'(\eta)$ diminishes. Influences of λ on velocity profiles $f'(\eta)$ and $g'(\eta)$ are displayed in figs. 4 and 5. It is clearly shown that $f'(\eta)$ enhances by increasing λ. In fact viscous forces are less effective rather then buoyancy forces. Opposite feature of $g'(\eta)$ is seen for high-

Table 1: Numerical data of surface heat transfer rate $-(1+Rd)\theta'(0)$ and surface mass transfer rate $-\phi'(0)$ for δ, Rd, γ_1, γ, Sr, and D_f when other parameters are fixed

δ	γ	Rd	γ_1	Sr	D_f	$(1+Rd)\theta'(0)$	$\phi'(0)$
0.0						0.10054	0.09181
0.3						0.10018	0.09151
1.0						0.09999	0.09150
	0.4					0.38052	0.08945
	1.0					0.50124	0.08420
	1.4					0.71584	0.07760
		0.0				0.09430	0.08964
		0.3				0.12612	0.90024
		0.6				0.75010	0.42019
			0.4			0.14561	0.93047
			0.8			0.14562	1.23450
			1.2			0.14563	1.34501
				0.0		0.09986	0.09171
				0.5		0.09990	0.08943
				0.9		0.09993	0.08805
					0.0	0.10037	0.09124
					0.4	0.09787	0.09129
					1.2	0.09636	0.09132

er λ. Figures 6 and 7 are sketched to visualize the behavior of N on $f'(\eta)$ and $g'(\eta)$. Here larger N result for an increment in $f'(\eta)$. For larger N both $g'(\eta)$ and momentum layer decayed. Curves of dimensionless $\theta(\eta)$ with change in M is elucidated in fig. 8. This figure reveals that $\theta(\eta)$ marginally increases as M is enhanced. It is well known fact that magnetic field intensity tends to produced drag force which resists the liquid motion and ultimately the thermal field is elevated. Figure 9 is drawn to see the characteristics of δ on $\theta(\eta)$. It is found that $\theta(\eta)$ is augmented for larger δ. Figure 10 is sketched to analyze behavior of Biot number γ on $\theta(\eta)$. It is concluded that $\theta(\eta)$ and related layer thickness are enhanced for larger γ. Figure 11 demonstrates to analyze the behavior of Rd on temperature $\theta(\eta)$. It is reported that $\theta(\eta)$ is

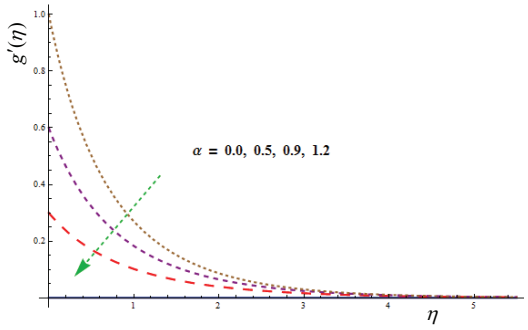

Figure 3. Impact of $g'(\eta)$ via α

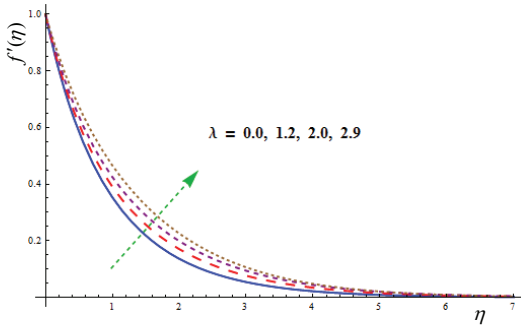

Figure 4. Impact of $f'(\eta)$ via λ

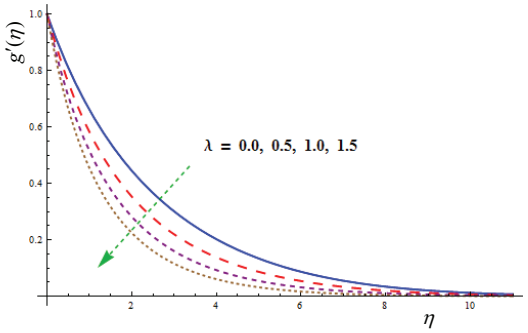

Figure 5. Impact of $g'(\eta)$ via λ

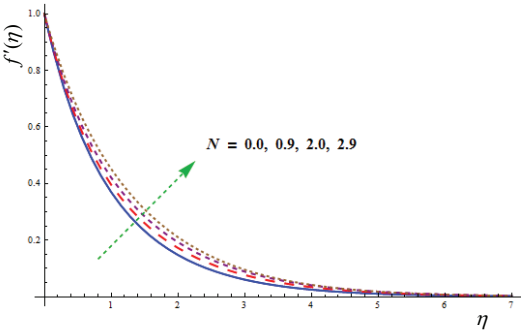

Figure 6. Impact of $f'(\eta)$ via N

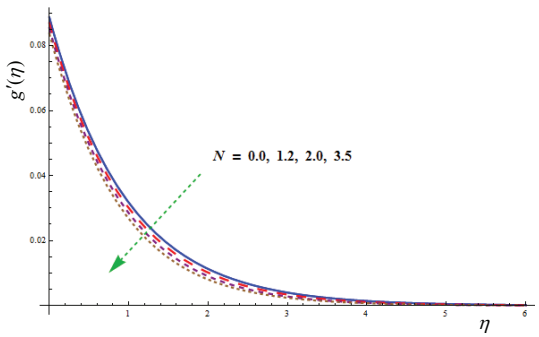

Figure 7. Impact of $g'(\eta)$ via N

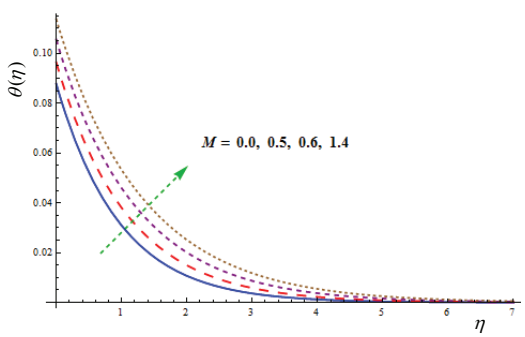

Figure 8. Impact of $\theta(\eta)$ via M

enhanced for higher Rd. Physically an increment in radiation promotes the heat flux which corresponds to rise in $\theta(\eta)$. Figure 12 elucidates that an increase in Prandtl number decays the thermal field. The fluid with higher Prandtl number is more viscous. The fluid with a higher viscosity has a lower temperature while the fluid with lower viscosity has higher temperature. Thus, an increase in Prandtl number leads to diminish $\theta(\eta)$. Impact of Soret number on $\theta(\eta)$ is depicted in fig. 13. There is reduction in $\theta(\eta)$ for higher Soret number. Temperature identifies increasing nature with intensity of Dufour number, see fig. 14. In fact Dufour number is involved in energy expression by concentration gradient. Therefore $\theta(\eta)$ is enhanced with higher concentration gradient. Figures 15 and 16 are drawn to see the impacts of γ_1 for generative

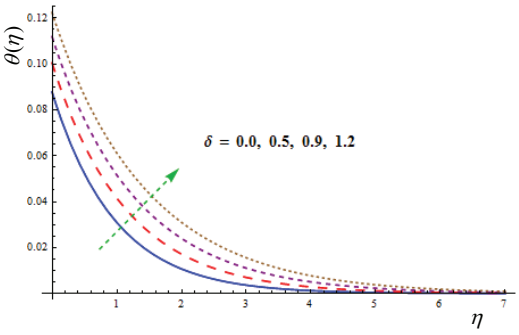

Figure 9. Impact of $\theta(\eta)$ via δ

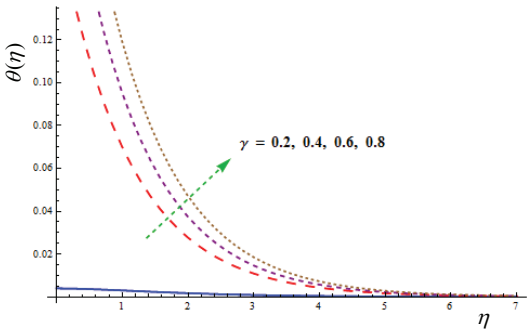

Figure 10. Impact of $\theta(\eta)$ via γ

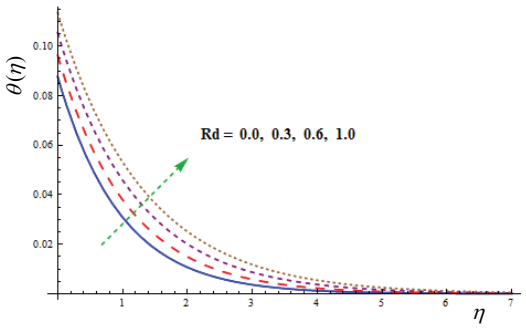

Figure 11. Impact of $\theta(\eta)$ via Rd

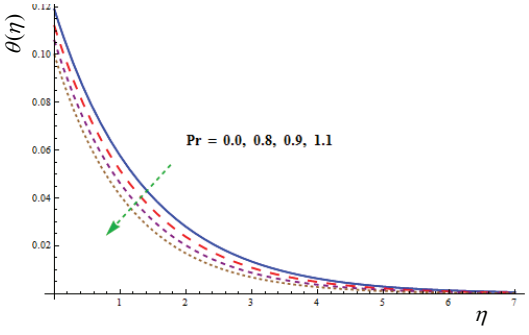

Figure 12. Impact of $\theta(\eta)$ via Pr

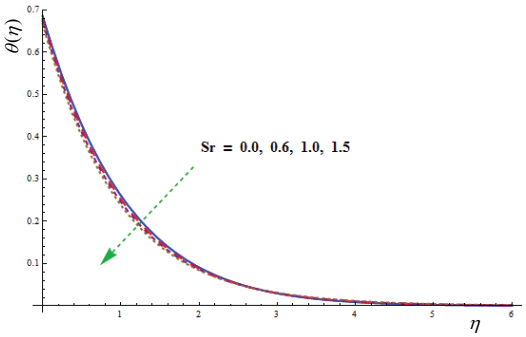

Figure 13. Impact of $\theta(\eta)$ via Sr

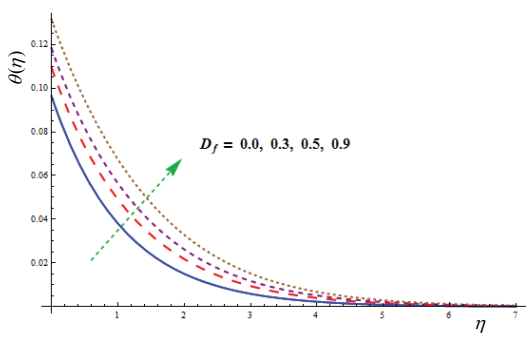

Figure 14. Impact of $\theta(\eta)$ via D_f

($\gamma_1 < 0$) and destructive ($\gamma_1 > 0$) chemical reactions for $\phi(\eta)$. Concentration field $\phi(\eta)$ reduces with increment in destructive chemical reaction ($\gamma_1 > 0$) while it enhances in case of ($\gamma_1 < 0$). Behavior of Schmidt number on $\phi(\eta)$ is presented in fig. 17. Schmidt number is the ratio of momentum diffusivity to the mass diffusivity higher Schmidt number lead to decay in mass diffusivity which in turn declines the concentration field. Figure 18 portrays the variation in $\phi(\eta)$ for various Soret number. Here $\phi(\eta)$ is an increasing function of Soret number. Figure 19 designates that higher Dufour number enhances the concentration and its related boundary-layer thickness. Tables 1 perceives numerical data of Nusselt and Sherwood numbers Rd, γ, γ_1, Sr, D_f, and δ. Here we concluded that Nusselt number enhances for Rd, γ, and Sr. It is also noted that Sherwood numbers decay via γ, δ, and Sr.

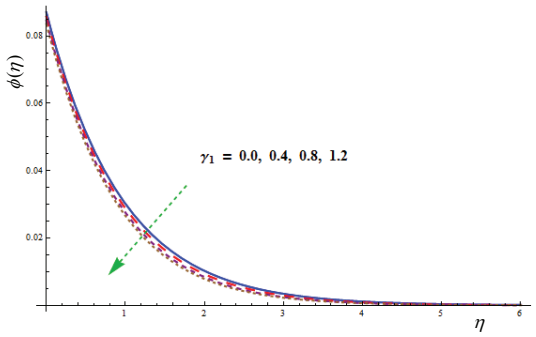

Figure 15. Impact of $\phi(\eta)$ via ($\gamma_1 \geq 0$)

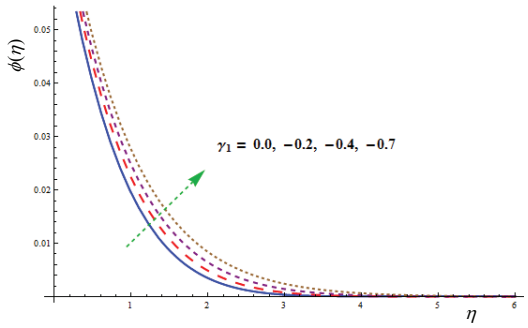

Figure 16. Impact of $\phi(\eta)$ via ($\gamma_1 \leq 0$)

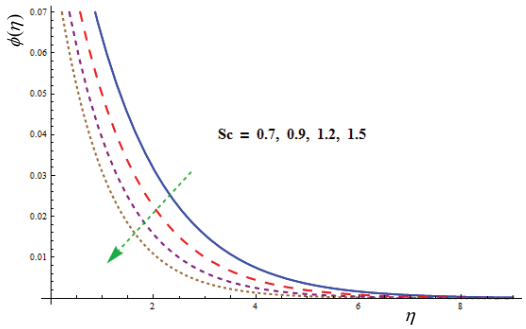

Figure 17. Impact of $\phi(\eta)$ via Sc

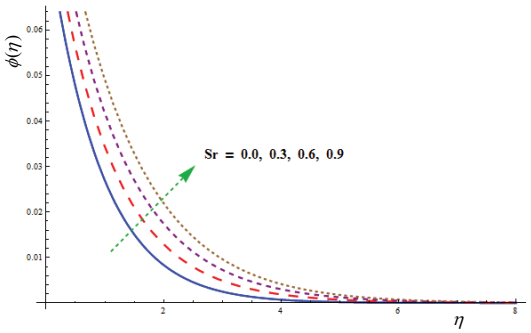

Figure 18. Impact of $\phi(\eta)$ via Sr

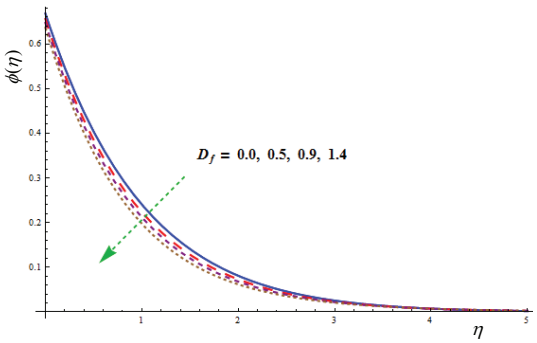

Figure 19. Impact of $\phi(\eta)$ via D_f

Closing remarks

Here we addressed the effects of Soret-Dufour and exponential space dependent internal heat source on MHD flow of viscoelastic liquid towards an exponentially stretched surface. Key results can be highlighted in the following bullets:

- Similar feature of velocity profiles are noticed for larger λ and N.
- Radiation and heat source variables improves the temperature field.
- Temperature is an increasing function of M.
- Features of Soret and Dufour numbers on temperature and concentration are quite reverse.
- Surface heat and mass transfer rates are augmented via δ.

References

[1] Crane, L. J., Flow Past a Stretching Plate, *Z. Angew Math. Phys., 21* (1970), 4, pp. 645-647
[2] Gupta, P. S., Gupta, A. S., Heat and Mass Transfer on a Stretching Sheet with Suction and Blowing, *Can. J. Chem. Eng., 55* (1977), 6, pp. 744-746
[3] Chen, C. K., Char, M. I., Heat Transfer of a Continuous Stretching Surface with Suction or Blowing, *J. Math. Anal. Appl., 135* (1988), 2, pp. 568-580
[4] Pop, I., Na, T. Y., Unsteady Flow Past a Stretching Sheet, *Mech. Res. Commun., 23* (1996), 4, pp. 413-422
[5] Kazem, S., *et al.*, Improved an Alytical Solutions to a Stagnation-Point Flow Past a Porous Stretching Sheet with Heat Generation, *J. Frankl Inst., 348* (2011), 8, pp. 2044-2058
[6] Hayat, T., *et al.*, MHD Flow of Powell-Eyring Nanofluid over a Non-Linear Stretching Sheet with Variable Thickness, *Results in Phys., 7* (2017), Apr., pp. 189-196
[7] Hussain, M., *et al.*, Radiation Effects on the Thermal Boundary Layer Flow of a Micropolar Fluid Towards a Permeable Stretching Sheet, *J. Frankl Inst., 350* (2013), 1, pp. 194-210
[8] Hayat, T., *et al.*, Flow of Magneto Williamson Nanoliquid Towards Stretching Sheet with Variable Thickness and Double Stratification, *Radiat. Phys. Chem., 152* (2018), Nov., pp. 151-157
[9] Pal, D., Mixed Convection Heat Transfer in the Boundary Layers on an Exponentially Stretching Surface with Magnetic Field, *Appl. Math. Comput., 217* (2010), 6, pp. 2356-2369
[10] Magyari, E., Keller, B., Heat and Mass Transfer in the Boundary Layers on an Exponentially Stretching Continuous Surface, *J. Phys. Appl. Phys., 32* (1999), 5, pp. 577-585
[11] Partha, M. K., *et al.*, Effect of Viscous Dissipation on the Mixed Convection Heat Transfer From an Exponentially Stretching Surface, *Heat Mass Transf., 41* (2005), 4, pp. 360-366
[12] Sajid, M., Hayat, T., Influence of Thermal Radiation on the Boundary Layer Flow Due to an Exponentially Stretching Sheet, *Int. Commun. Heat Mass Transf., 35* (2008), 3, pp. 347-356
[13] Hayat, T., *et al.*, Magnetohydrodynamic (MHD) Three-Dimensional Flow of Second Grade Nanofluid by a Convectively Heated Exponentially Stretching Surface, *J. Mol. Liq., 220* (2016), Aug., pp. 1004-1012
[14] Rashidi, M. M., *et al.*, Simultaneous Effects of Partial Slip and Thermal-Diffusion and Diffusion-Thermo on Steady MHD Convective Flow Due to a Rotating Disk, *Comm. Nonl. Sci. Numer. Simulation, 16* (2011), 11, pp. 4303-4317
[15] Cheng, C. Y., Soret and Dufour Effects on Mixed Convection Heat and Mass Transfer From a Vertical Wedge in a Porous Medium with Constant Wall Temperature and Concentration, *Trnsp. Porous Med., 94* (2012), 1, pp. 123-132
[16] Turkyilmazoglu, M., Pop, I., Soret and Heat Source Effects on the Unsteady Radiative MHD Free Convection Flow from an Impulsively Started Infinite Vertical Plate, *Int. J. Heat Mass Transfer, 55* (2012), 25-26, pp. 7635-7644
[17] Hayat, T., *et al.*, Stagnation Point Flow of Hyperbolic Tangent Fluid with Soret-Dufour Effects, *Results Phys., 7* (2017), July, pp. 2711-2717
[18] Hayat, T., *et al.*, Radiative Three-Dimensional Flow with Soret and Dufour Effects, *Int. J. Mech. Sci., 133* (2017), Nov., pp. 829-837
[19] Turkyilmazoglu, M., The Analytical Solution of Mixed Convection Heat Transfer and Fluid Flow of a MHD Viscoelastic Fluid over a Permeable Stretching Surface, *Int. J. Mech. Sci., 77* (2013), Dec., pp. 263-268
[20] Grosan, T., *et al.*, Mixed Convection Boundary-Layer Flow on a Horizontal Flat Surface with a Convective Boundary Condition, *Meccanica, 48* (2013), 9, pp. 2149-2158

[21] Das, S., *et al.*, Magnetohydrodynamic Mixed Convective Slip Flow over an Inclined Porous Plate with Viscous Dissipation and Joule Heating, *Alex. Eng. J., 54* (2015), 2, pp. 251-61
[22] Imtaiz, M., *et al.*, Mixed Convection Flow of Nanofluid with Newtonian Heating, *Eur. Phys. J. Plus, 129* (2014), May, 97
[23] Hayat, T., *et al.*, Three-Dimensional Mixed Convection Flow of Sisko Nanoliquid, *Int. J. Mech. Sci., 133* (2017), Nov., pp. 273-282
[24] Zheng, L., *et al.*, Flow and Radiation Heat Transfer of a Nanofluid over a Stretching Sheet with Velocity Slip and Temperature Jump in Porous Medium, *J. Franklin. Inst., 350* (2013), 5, pp. 990-1007
[25] Sheikholeslami, M., *et al.*, Effect of Thermal Radiation on Magnetohydrodynamics Nanofluid Flow and Heat Transfer by Means of Two Phase Model, *J. Magn. Magn. Mater., 374* (2015), Jan., pp. 36-43
[26] Abbasi, F. M., *et al.*, Mixed Convection Flow of Jeffrey Nanofluid with Thermal Radiation and Double Stratification, *J. Hydrodynamics Ser. B, 28* (2016), 5, pp. 840-849
[27] Hayat, T., *et al.*, MHD Mixed Convection Flow of Third Grade Liquid Subject to Non-Linear Thermal Radiation and Convective Condition, *Results Phys., 7* (2017), Aug., pp. 2804-2811
[28] Hayat, T., *et al.*, Simultaneous Effects of Non-Linear Mixed Convection and Radiative Flow Due to Riga-Plate with Double Stratification, *J. Heat Transfer, 140* (2018), 10, 102008
[29] Salem, A. M., El-Aziz, M. A., MHD Mixed Convection and Mass Transfer from a Vertical Stretching Sheet with Diffusion of Chemically Reactive Species and Space or Temperature-Dependent Heat Source, *Can. J. Phys., 85* (2007), 4, pp. 359-373
[30] Mahanthesh, B., *et al.*, Cattaneo-Christov Heat Flux on UCM Nanofluid Flow Across a Melting Surface with Double Stratification and Exponential Space Dependent Internal Heat Source, *Informatics in Medicine Unlocked, 9* (2017), May, pp. 26-34
[31] Zaigham Zia, Q. M., *et al.*, Cross Diffusion and Exponential Space Dependent Heat Source Impacts in Radiated Three-Dimensional (3D) Flow of Casson Fluid by Heated Surface, *Results Phys., 8* (2018), Mar., pp. 1275-1282
[32] Liao, S. J., On the Homotopy Analysis Method for Nonlinear Problems, *Appl. Math. Comput., 147* (2004), 2, pp. 499-513
[33] Dehghan, M., *et al.*, Solving Nonlinear Fractional Partial Differential Equations Using the Homotopy Analysis Method, *Numer. Meth. Partial Diff. Eq., 26* (2010), July, pp. 448-479
[34] Bansod, V., Jadhav, R., Effect of Double Stratification on Mixed Convection Heat and Mass Transfer from a Vertical Surface in a Fluid-Saturated Porous Medium, *Heat Transfer Asian Res., 39* (2010), 6, pp. 378-395
[35] Hayat, T., *et al.*, MHD Stratified Nanofluid Flow by Slandering Surface, *Phys. Scr., 93* (2018), 11, 5701
[36] Abbasbandy, S., *et al.*, Numerical and Analytical Solutions for Falkner-Skan Flow of MHD Oldroyd-B Fluid, *Int. J. Numer. Methods Heat Fluid Flow, 24* (2014), 2, pp. 390-401
[37] Hayat, T., *et al.*, Impact of Temperature Dependent Heat Source and Nonlinear Radiative Flow of Third Grade Fluid with Chemical Aspects, *Thermal Science*, (2018), On-line first, https//doi.org/10.2298/TSCI180409245H
[38] Ellahi, R., *et al.*, Shape Effects of Nanosize Particles in Cu-H_2O Nanofluid on Entropy Generation, *Int. J. Heat Mass Transfer, 81* (2015), Feb., pp. 449-456
[39] Hayat, T., *et al.*, Double Stratified Flow of Nanofluid Subject to Temperature Based Thermal Conductivity and Heat Source, *Thermal Science*, (2018), On-line first, https//doi.org/10.2298/TSCI180121242H
[40] Turkyilmazoglu, M., An Effective Approach for Evaluation of the Optimal Convergence Control Parameter in the Homotopy Analysis Method, *Filomat, 30* (2016), 6, pp. 1633-1650
[41] Hayat, T., *et al.*, A Revised Model for Stretched Flow of Third Grade Fluid Subject to Magneto Nanoparticles and Convective Condition, *J. Mol. Liq., 230* (2017), Mar., pp. 608-615
[42] Ahmad, I., *et al.*, Series Solutions for the Radiation-Conduction Interaction on Unsteady MHD Flow, *J. Porous Media, 14* (2011), 10, pp. 927-941
[43] Ullah, I., *et al.*, Thermally Radiated Squeezed Flow of Magneto-Nanofluid between Two Parallel Disks with Chemical Reaction, *J. Therm. Anal. Calorim., 135* (2018), 2, pp. 1021-1030

Paper submitted: December 29, 2017
Paper revised: September 16, 2018
Paper accepted: September 26, 2018